International Journal of Marine Engineering Innovation and Research, Vol. 11(2), Jun. 2026. 426-436
(pISSN: 2541-5972, eISSN: 2548-1479)

Effect of Bilge Keel on The Resistance Characteristic of Fishing Vessels in Benoa: A CFD Simulations Study

Tiara Asya Da Rosta[1*], Mohammad Ridwan Utina[2], Nanang Setiyobudi[3], Dian Purnamasari[4], Wiwin Sulistyawati[5]

(Received: 15 April 2026 / Revised: 18 April 2026 / Accepted: 21 April 2026 / Available Online: 3 June 2026)

***Abstract*—** Bilge keels are commonly utilized on fishing vessels to improve stability; nevertheless, their effect on resistance in calm waters for specific hull types remains insufficiently documented. This research examines the resistance characteristics of a 33.5 m Indonesian tuna longline fishing vessel, both with and without bilge keels, employing a validated Computational Fluid Dynamics (CFD) methodology. Simulations utilized the steady state Reynolds Averaged Navier Stokes (RANS) equations and were validated against towing tank data at velocities of 3, 6, and 9 knots. The results indicate that the total resistance increases non-linearly with speed for both configurations. The bilge keel equipped configuration consistently produces lower total resistance, with approximately 18% reduction at the design speed of 6 knots. Qualitative flow field analysis associates this trend with a redistribution of near wall velocity and a more gradual pressure recovery in the aft bilge region. These findings suggest that, within the limits of the investigated configuration, bilge keels may influence hydrodynamic performance beyond their conventional role in stability, providing a reference for the design of energy efficient fishing vessels.

Keywords— Fishing Vessel, Bilge Keel, Resistance, CFD

Corresponding Author: 2210313039@mahasiswa.upnvj.ac.id

I. INTRODUCTION

To design modern ships, a detailed understanding is required of how the hull shape, appendages, and the flow field around the ship interact. Even modest changes to an object's shape, such as adding passive appendages, can significantly affect the development of the boundary layer, the pressure distribution, and the wake characteristics, which, in turn, can affect total resistance and overall energy efficiency [1]. This issue has become more essential as maritime decarbonization has become more important. Lowering hydrodynamic resistance is a key approach to reducing fuel use and greenhouse gas emissions [2]. For vessels that do a lot of work, such as fishing boats, even small changes in resistance can have a notable effect on performance and energy use [3].

Fishing boats are a unique type of displacement ship. They usually have full hulls and operate at low to moderate Froude numbers. Bilge keels are among the most common appendages. They are mostly employed to make boats more stable and safer to operate [4]. But their effect on calm water resistance remains complicated and not entirely understood. Although increased wetted surface area and appendage induced drag are typically associated with increased resistance, prior research has demonstrated that bilge keels can also alter local flow dynamics, pressure distribution, and separation characteristics, resulting in fluctuations in total resistance contingent on their geometry and configuration [5], [6].

In the specific context of bilge keels on full bodied hulls, Putra et al. [5] conducted a CFD study on a traditional phinisi boat. They reported that the direction and magnitude of the resistance change strongly depend on the bilge keel arrangement, indicating that the overall hydrodynamic outcome is not uniquely determined by the appendage's presence alone. Oyuela et al. [7] subsequently showed that the stern flow region of fishing vessels, being characterized by full forms and relatively blunt aft geometry, tends to respond differently to appendages than slender displacement hulls, which implies that bilge keel performance is sensitive to the host hull geometry. From an appendage optimization standpoint, Yu et al. [3] demonstrated for a coastal fishing vessel that stern appendage modifications can improve overall resistance when the appendage interacts favorably with the aft flow field. Within the scope of Indonesian fishing vessel research, Hamka et al. [8] evaluated the technical performance of outrigger fishing vessels at Palabuhanratu. They showed that hull form modifications substantially affect the resistance, stability, and seakeeping response of locally operating working boats, underscoring the need for geometry specific hydrodynamic assessment of appendage equipped fishing vessels. In a complementary context, Harifuddin et al. [9] employed a CFD framework validated against

Tiara Asya Da Rosta, Department of Naval Engineering, Universitas Pembangunan Nasional Veteran Jakarta, Jakarta 12450, Indonesia E-mail: 2210313039@mahasiswa.upnvj.ac.id
Mohammad Ridwan Utina, is with Research Center for Hydrodynamics Technology, National Research and Innovation Agency Republic of Indonesia, Surabaya, 60112, Indonesia E-mail: muha009@brin.go.id
Nanang Setiyobudi, is with Research Center for Hydrodynamics Technology, National Research and Innovation Agency Republic of Indonesia, Surabaya, 60112 E-mail: nana025@brin.go.id
Dian Purnamasari, is with Research Center for Hydrodynamics Technology, National Research and Innovation Agency Republic of Indonesia, Surabaya, 60112 Indonesia E-mail: dian010@brin.go.id
Wiwin Sulistyawati, Department of Naval Engineering, Universitas Pembangunan Nasional Veteran Jakarta, Jakarta 12450, Indonesia E-mail: wiwinsulistyawati@upnvj.ac.id

the Holtrop empirical method to evaluate the effect of a rudder bulb installation on an anchor handling vessel, demonstrating that appendage induced changes in overall performance are inherently speed dependent. Taken together, these results indicate that the resistance response of a fishing vessel hull to bilge keel installation is highly case specific and cannot be generalized from a single reference configuration, particularly when the host hull geometry differs from those studied in the existing literature.

From a methodological standpoint, ship resistance prediction and flow characteristic analysis have extensively used Computational Fluid Dynamics (CFD), based on the Reynolds Averaged Navier Stokes (RANS) equations. Validated RANS based CFD is a dependable technique for comparative hydrodynamic studies, as it can precisely capture viscous flow, free surface effects, and appendage induced resistance, according to studies by I. Sulovsky et al. [10] and E. Begovic et al. [11].

Despite these advances, two practical gaps remain. First, validated hydrodynamic evidence for Indonesian tuna longline fishing vessels whose geometry is reconstructed directly from field survey data is not readily available in the open literature [7], which limits the direct applicability of conclusions drawn from generalized hull forms to local vessel design practice. Second, although CFD based resistance assessments of appendage equipped hulls have been reported, dedicated studies that combine towing tank based validation with a flow field based interpretation of the resistance behavior for this specific class of working vessel remain scarce. These two gaps together motivate a numerical investigation whose outcomes can be directly referenced to Indonesian fishing vessel design practice.

Accordingly, the main problem addressed in this study is the lack of validated hydrodynamic evidence regarding whether bilge keel installation increases or reduces resistance for realistic fishing vessel hull forms. The novelty of this study lies in the integration of a field survey based hull model with a validated RANS based CFD approach, supported by direct comparison with towing tank data [10], [11]. In addition, this study provides a flow based interpretation of resistance behavior by linking global resistance trends with local velocity distributions and pressure recovery in the bilge region.

Therefore, this study aims to investigate the effect of bilge keel installation on the resistance characteristics of a tuna longline fishing vessel using a validated CFD framework. The findings are expected to provide a more reliable basis for evaluating the hydrodynamic role of bilge keels beyond their conventional function in vessel stability, particularly for fishing vessels operating in Indonesian waters.

II. METHOD

A. Ship Data and 3D Model Generation

The vessel considered in this study is a tuna longline fishing vessel with a gross tonnage of 265 GT, representative of medium scale fishing vessels operating in Indonesian waters. The hull form was developed based on principal dimensions and geometric characteristics obtained from direct field survey data conducted in the Benoa fishing port area, Bali, and the reconstructed hull geometry reflects the operational and environmental characteristics of tuna longline vessels, including their representative hull form and service profile. The hull geometry and corresponding lines plan of the vessel are presented in Figure 1.

The principal dimensions of the vessel are summarized in Table 1. In the present study, both the experimental reference data and the numerical simulations were based on a ship model at a geometric scale ratio of 1:9.685. All geometric reconstruction, appendages installation, and resistance analyses were performed on the scaled model geometry to ensure consistency between the Computational Fluid Dynamics (CFD) simulations and the Experimental Fluid Dynamics (EFD) reference data used for validation.

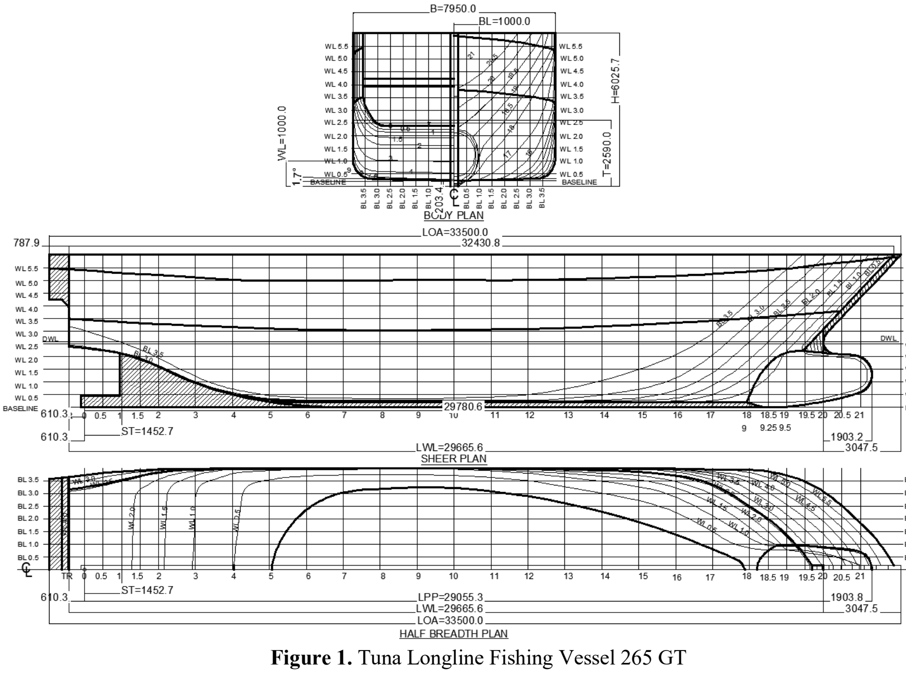

Figure 1. Tuna Longline Fishing Vessel 265 GT

TABLE 1.
PRINCIPAL DIMENSIONS OF THE FULLSCALE VESSEL AND SHIP MODEL

Dimension	Full scale Vessel	Ship Model	Unit
LOA	33.500	3.459	m
LPP	29.054	3	m
B	7.950	0.821	m
H	4.060	0.622	m
T	2.590	0.267	m
Displacement (Δ)	415.6	439.1	ton
Gross Tonage	265	-	ton

The hull geometry of the fishing vessel was reconstructed through a multistage modeling procedure to ensure consistency with the scaled principal dimensions and hydrostatic characteristics. The original lines plan was first corrected and refined in AutoCAD to achieve precise agreement with the target model scale principal particulars. The refined sectional data were subsequently imported into Maxsurf Modeler Advanced for three-dimensional hull generation and surface fairing, resulting in a smooth and hydrodynamically consistent hull geometry representative of the intended vessel form at model scale.

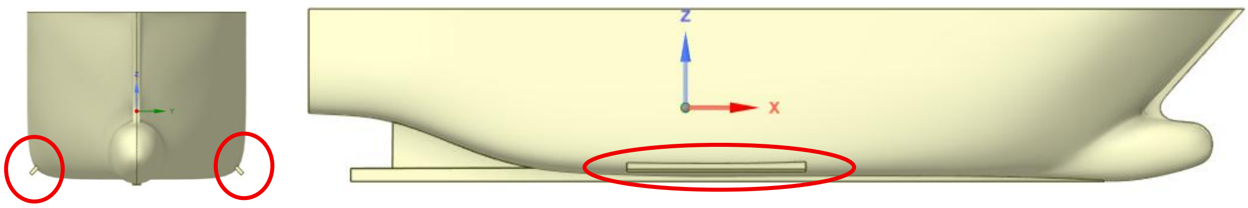

Figure 2. 3D Modeling of Hull with Bilge Keel

TABLE 2.
PRINCIPAL DIMENSION OF THE BILGE KEEL

Dimension of The Bilge Keel	Value	Unit
Longitudinal Position	5	mm
Length	667	mm
Height	10	mm

The Maxsurf generated hull surface was subsequently exported to SpaceClaim for final geometric processing, where surface refinement and solid modeling operations were performed to obtain a watertight, fully closed solid model suitable for numerical simulation. The resulting geometry represents the bare hull configuration, which served as the baseline model for all resistance simulations and numerical validation procedures.

Following the finalization of the bare hull geometry, the bilge keel was introduced as a geometric modification applied directly to the three-dimensional hull in Figure 2. The bilge keel dimensions adopted in this study were selected based on experimental investigations of low aspect ratio appendages conducted by van der Kolk et al. (2021) [12], in which systematic variations of bilge keel length, height, and longitudinal position were evaluated on displacement type hull forms with pronounced bilge. The selected bilge keel configuration (B-P2-L2-H1), as summarized in Table 2, falls within the hydrodynamically effective dimensional range for hull forms comparable to the present fishing vessel, allowing effective interaction with the developed boundary layer while limiting excessive form drag.

B. Numerical Methods

The resistance characteristics of the fishing vessel were evaluated using CFD based on the Reynolds Averaged Navier Stokes (RANS) equations. This approach is well established for predicting viscous free surface flow and ship resistance under steady forward motion [13]. In the present study, the incompressible turbulent flow around the hull was governed by the continuity and momentum conservation equations

$$\nabla \cdot u = 0 \qquad (1)$$

$$\rho\left(\frac{\partial u}{\partial t} + u \cdot \nabla u\right) = -\nabla p + \nabla \cdot [(\mu + \mu_t)(\nabla u + \nabla u^T)] \qquad (2)$$

Where $\mathbf{u}$ is the velocity vector p is the pressure, ρ is the fluid density, μ is the dynamic viscosity, and μ_t is the turbulent eddy viscosity is introduced by the turbulence model.

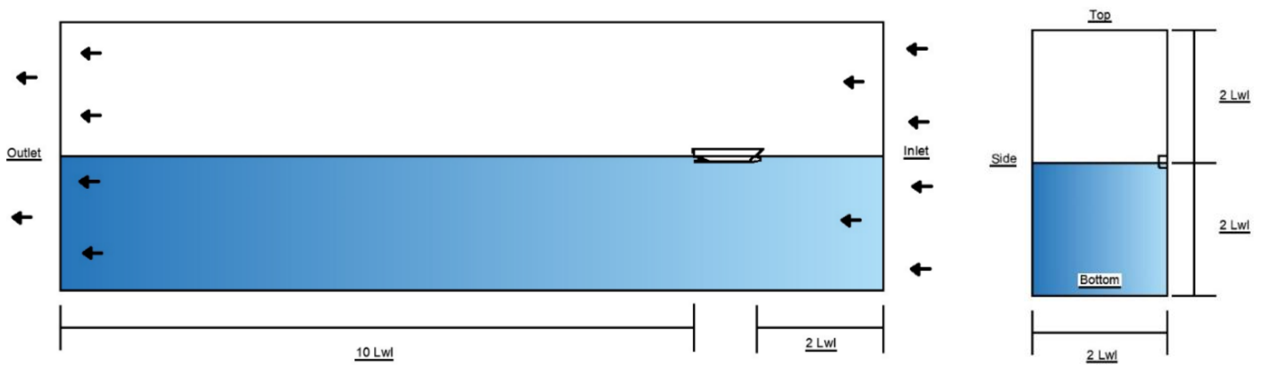

Figure 3. Domain

The computational domain was defined to represent open water conditions, with the vessel advancing in calm water, as illustrated in Figure 3. The upstream boundary was positioned approximately 2L ahead of the forward perpendicular. In contrast, the downstream boundary was extended 10L aft of the aft perpendicular to allow adequate wake development and minimize blockage effects. The lateral and bottom boundaries were located approximately 2L from the hull to reduce artificial confinement. A two phase air water formulation was adopted using the Volume of Fluid (VOF) method to capture free surface effects and wave generation. At the inlet, a uniform velocity corresponding to each prescribed simulation speed was imposed, while a pressure outlet condition was applied at the outlet boundary. A no slip wall condition was imposed on the hull surface, and far field conditions were assigned to the remaining outer surfaces. A symmetry plane was applied along the vessel centerline to reduce computational cost while preserving flow symmetry [14].

Simulations were performed under steady state conditions to evaluate the total resistance (R_T) for each hull configuration. A steady state Reynolds averaged Navier Stokes (RANS) formulation was adopted for resistance prediction with turbulence closure provided by the SST k-ω model due to its established capability in resolving near wall viscous flow and flow regions affected by adverse pressure gradients and separation [15]. The choice of a mesh based RANS framework is consistent with recent practice in ship resistance analysis in the marine engineering literature, including both conventional mesh based approaches and emerging mesh free alternatives such as smoothed particle hydrodynamics [16], where comparison against towing tank data remains a standard verification step. This numerical setup was selected to ensure consistent and reliable assessment of resistance variations associated with bilge keel installation.

A mesh convergence study was conducted to ensure the reliability of the computed resistance results. An unstructured mesh system was employed, consisting of prismatic elements in the boundary layer region and tetrahedral elements in the remaining computational domain. Mesh refinement was performed iteratively through multiple levels to assess solution sensitivity to grid density [17]. The element size was systematically varied for both the hull surface and the surrounding domain, ranging from relatively coarse to finer resolutions.

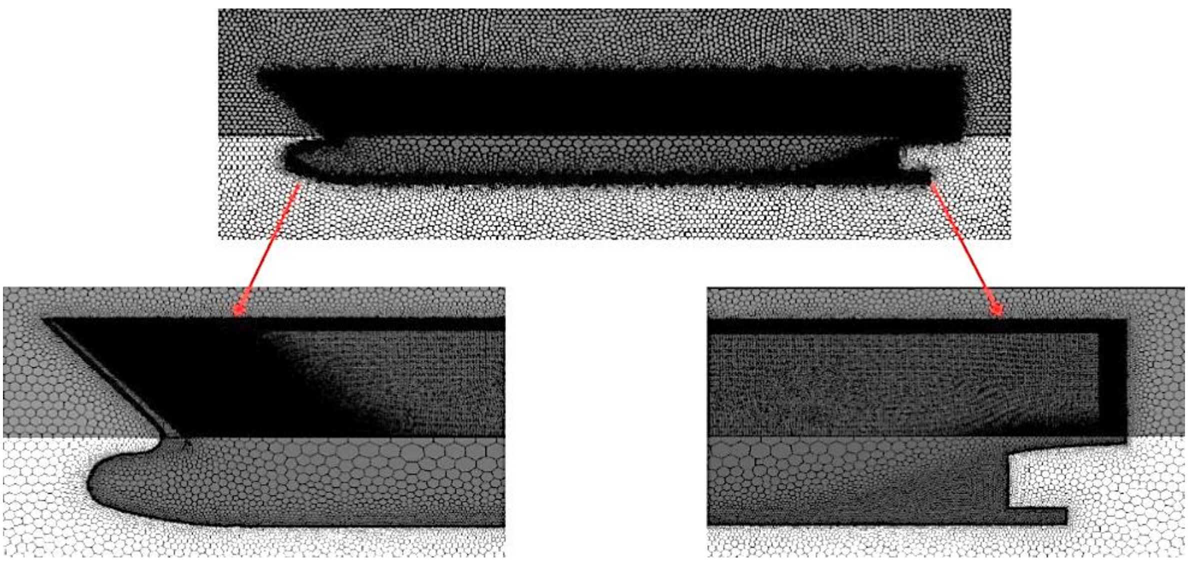

Figure 4. Mesh Configuration on Bare Hull

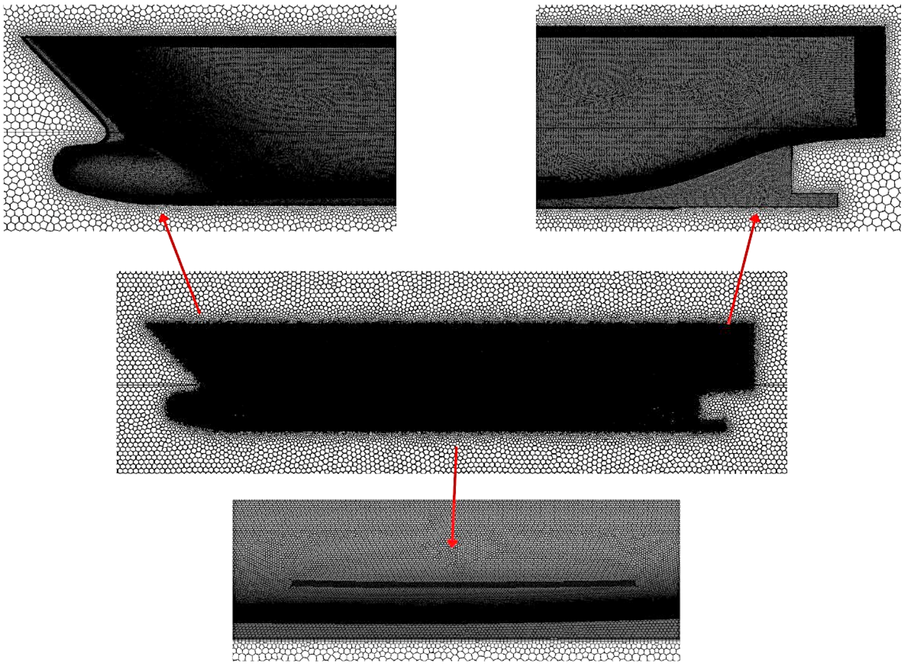

Figure 5. Mesh Configuration on Bilge Keel

Grid convergence was considered achieved when further mesh refinement produced only marginal changes in the computed resistance, corresponding to a domain element size of approximately 0.03 and a refined near hull mesh size of approximately 0.005. The resulting mesh distributions adopted for the numerical simulations are presented in Figure 4 for the bare hull configuration and Figure 5 for the hull with the bilge keel. A hybrid wall treatment approach was employed, with the first near wall grid point corresponding to a non-dimensional wall distance of $y^+ \approx 15–30$, and localized regions reaching approximately $y^+ \approx 90$. This range is generally considered acceptable for wall function based RANS simulations in resistance prediction studies [18].

C. Resistance Calculation Procedure

The hydrodynamic performance of the vessel is quantified by the total resistance acting on the hull during steady forward motion. In a viscous free surface flow, the total resistance arises from the combined effects of pressure forces and viscous shear stresses distributed over the wetted hull and appendage surfaces. Within a CFD framework, this quantity is obtained directly from surface force integration and has been shown to provide accurate predictions when properly validated against experimental data. Mathematically, the total resistance is expressed as follows:

$$R_T = \frac{1}{2}\rho V^2 S C_T \tag{3}$$

where R_T is the total resistance force extracted directly from the CFD solution through surface force integration, ρ is the water density, V is the ship forward speed, and S is the wetted surface area. This non-dimensional formulation allows resistance values obtained at different operating speeds to be compared on a consistent hydrodynamic basis [19].

For comparison between operating conditions and hull configurations, the total resistance is nondimensionalized using the total resistance coefficient.

$$C_T = C_F + C_R \tag{4}$$

The frictional resistance coefficient C_F represents the viscous shear contribution along the wetted surface and is evaluated using the ITTC 1957 correlation line.

$$C_F = \frac{0.075}{(log_{10}Re - 2)^2} \tag{5}$$

where the Reynolds number Re is defined as

$$Re = \frac{\rho V L_{wl}}{\mu} \tag{6}$$

where Re is the Reynolds number based on the characteristic length water line, and μ is the dynamic viscosity. This formulation provides a widely used reference skin friction level for both experimental and numerical resistance analyses.

The residual resistance coefficient C_R accounts for resistance components not captured by skin friction alone and is expressed as

$$C_R = C_W + C_{V,\text{hull}} + C_{V,\text{app}} \tag{7}$$

where C_W denotes the wave making resistance which arises from free surface deformation and wave generation, C_V contributions associated with hull geometry and appendages.

To account for three-dimensional viscous effects induced by hull geometry, such as flow curvature, pressure gradients, and local separation, a form factor $(1+k)$ is applied to the bare hull friction coefficient, yielding.

$$C_{V,\text{hull}} = (1 + k)\, C_F \tag{8}$$

The use of the form factor is well established in resistance decomposition theory. It reflects the additional viscous losses not captured by flat plate friction alone, particularly in full bodied working vessels [20]. For appendages such as bilge keels, viscous losses are further amplified by their slender geometry, leading edge separation, and operation within the disturbed boundary layer of the hull. These effects are commonly represented using a larger effective form factor $(2+k)$, such that the viscous resistance contribution of appendages becomes

$$C_{V,\,app} = (2 + k)\, C_{F,app} \tag{9}$$

where $C_{F,\text{app}}$ is calculated based on the appendage Reynolds number and wetted surface area. This formulation reflects the disproportionately higher viscous and form drag generated by appendages, which are not adequately represented by hull based friction models [21].

To ensure the reliability of the numerical predictions, the bare hull resistance results were validated against secondary towing tank data provided by the National Research and Innovation Agency (BRIN), Indonesia, derived from experimental testing of the same vessel model previously reported by Purnamasari et al. (2025) [22]. Although the original experimental dataset includes various operating conditions, three key validation speeds were selected at 3, 6, and 9 knots. These speeds correspond to low speed operation with a Froude number of 0.090, the vessel's operational design speed with a Froude number of 0.181, and a higher service speed with a Froude number of 0.271. These speeds are representative of tuna longline fishing vessels operating in the Benoa waters and were considered sufficient to establish a comprehensive characterization of the vessel's baseline resistance behavior across its practical operational range. The validated bare hull CFD setup was subsequently adopted as the numerical basis for the comparative assessment of the bilge keel equipped configuration [23].

III. RESULT AND DISCUSSION

A. Validation

The reliability of the present CFD framework was first assessed by validating against secondary towing tank data from the National Research and Innovation Agency (BRIN), Indonesia. The experimental dataset covers the bare hull configuration at three representative speeds of 3, 6, and 9 kn (Fn = 0.090, 0.181, and 0.271), and was used as a reference for numerical validation.

Figure 6. EFD Bare Hull, 9 kn

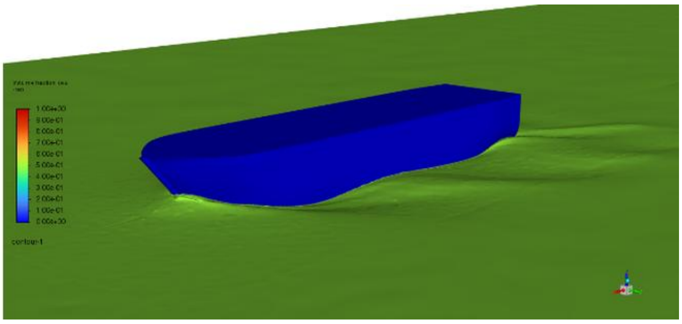

Figure 7. CFD Bare Hull, 9 kn

Validation was conducted at two levels: qualitative comparison of free surface wave patterns and quantitative comparison of total resistance. The wave elevation contours from both the towing tank measurements and the CFD simulations are presented in Figures 6 and 7. A side by side comparison shows strong agreement in the overall wave topology across all investigated speeds. The bow wave system, including the diverging wave crests and shoulder wave formation, is consistently reproduced in the numerical results. Similarly, the wave trough along the midship region and the stern wave pattern exhibit comparable spatial characteristics between the two datasets. The progressive increase in wave elevation with increasing speed is also consistently captured, reflecting the expected behavior of displacement hulls. A slight underprediction of wave amplitude near the stern at 9 knots is observed, which may be attributed to the steady state RANS formulation that has limited capability in resolving unsteady wake structures at higher Froude numbers. This qualitative agreement provides a basis for further quantitative validation by comparing total resistance values.

The quantitative validation is presented in Figure 8, which compares the total resistance values obtained from BRIN towing tank measurements with those from CFD predictions at the three reference speeds. The numerical results reproduce the same nonlinear increasing trend with speed observed in the experimental data, consistent with the expected behavior of displacement hulls in calm water.

At the vessel's design speed of 6 kn, the difference between the CFD prediction and the experimental result is 3.3%, indicating close agreement within the range generally considered acceptable for steady state RANS based resistance simulation. At 9 kn, the deviation increases slightly to 5.6%, while still maintaining reasonable agreement across the upper operating range.

A larger deviation of 62% is observed at 3 knots. However, this discrepancy is associated with the low speed flow regime, where the total resistance is relatively small and dominated by viscous effects. Under such conditions, small absolute differences can lead to large percentage deviations. Since this speed falls below the vessel's typical operational range, the observed deviation is not considered representative of the model's performance within the intended analysis range.

The agreement obtained at the representative operating speeds, together with the previously observed consistency in wave patterns, indicates that the present CFD framework provides a sufficiently reliable basis for comparative resistance analysis. The validated numerical setup is therefore used in the following section to examine the resistance characteristics of bare hull and bilge keel configurations.

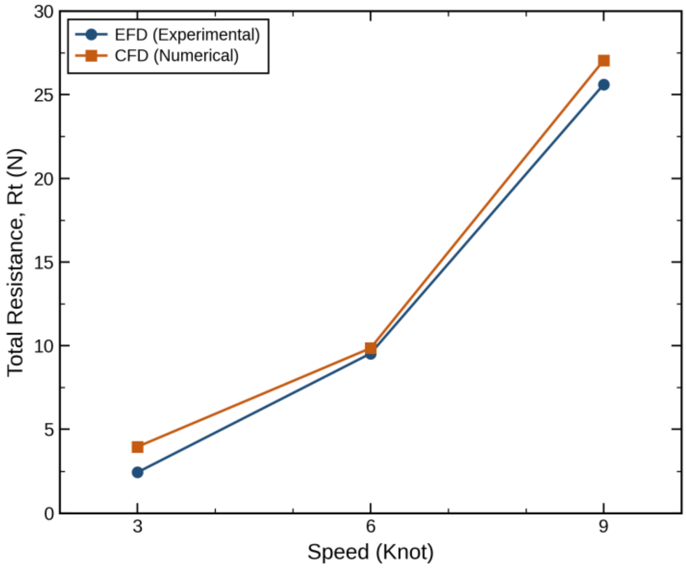

Figure 8. Comparison of EFD and CFD Analysis on Bare Hull

B. Effect of The Bilge Keel on Total Resistance.

Upon confirming the reliability of the numerical framework, the subsequent analysis presents a detailed comparison of the resistance characteristics between the bare hull and bilge keel configurations. This section examines the total resistance (RT) for both configurations across the full speed range from 3 to 9 knots. It delves into flow and pressure contours, providing insights into the underlying fluid dynamics and their influence on the observed resistance trends.

Having established the reliability of the numerical framework, the resistance performance of both hull configurations was evaluated over the full speed range from 3 kn to 9 kn. The total resistance curves for the bare hull and the bilge keel equipped hull are presented in Figure 9 and Table 3. Both configurations exhibit the expected nonlinear increase in resistance with increasing speed, reflecting the combined effects of viscous and wave making components as the Froude number increases. The smooth and monotonic behavior of the curves indicates stable numerical performance across the investigated range.

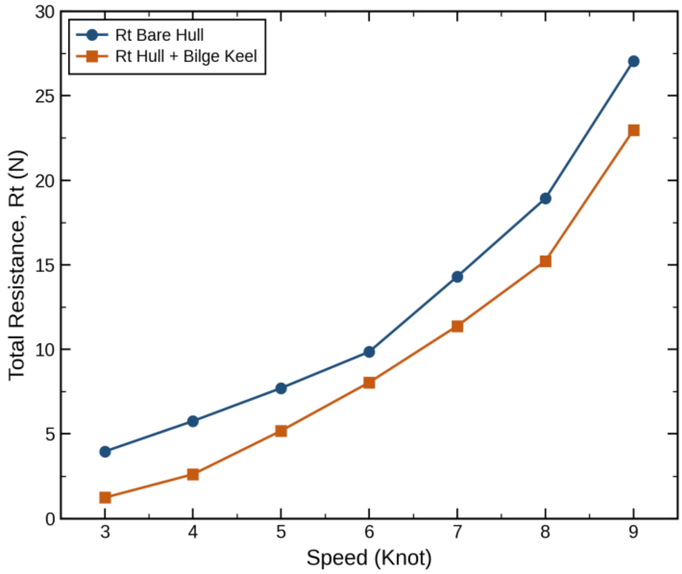

Figure 9. Comparison of Resistance Total of Bare Hull and Bilge Keel on CFD Analysis

TABLE 3.
DATA COMPARISON OF RESISTANCE TOTAL OF BARE HULL AND BILGE KEEL ON CFD ANALYSIS

Speed (Knot)	Froude Number	RT Bare Hull (N)	RT Bilge Keel (N)
3	0.090	3.96	1.23
4	0.121	5.75	2.60
5	0.151	7.70	5.18
6	0.181	9.85	8.04
7	0.211	14.30	11.38
8	0.241	18.92	15.21
9	0.271	27.05	22.96

A notable result of the simulations is that the bilge keel equipped hull consistently produces lower total resistance than the bare hull at all investigated speeds. At the design speed of 6 knots, the resistance decreases from 9.85 N for the bare hull to 8.04 N for the bilge keel configuration, corresponding to a reduction of approximately 18%. A similar trend is observed at 9 knots, where the bilge keel configuration maintains lower resistance than the bare hull.

This observation is of particular interest because it contrasts with the conventional expectation that bilge keel installation introduces an additional drag penalty due to the increased wetted surface area and appendage induced drag. Within the limits of the present numerical framework, the predicted trend suggests that the additional wetted surface does not uniquely determine the hydrodynamic outcome but is also influenced by the appendage's modification of the near hull flow field. The subsequent subsections examine the associated velocity and pressure distributions to provide an initial, flow based interpretation of this behavior, rather than to claim a definitive mechanistic explanation for the magnitude of the observed reduction.

These observations are consistent with previous studies reporting that low aspect ratio appendages may, under certain geometric conditions, produce favorable hydrodynamic interactions with the developing boundary layer. It should be noted, however, that the experimental validation in the present study was performed only for the bare hull configuration. In contrast, the bilge keel equipped configuration was evaluated using the same validated numerical setup without an independent experimental counterpart. The predicted reduction trend is therefore interpreted as a numerical outcome supported by a validated bare hull setup, rather than as an experimentally confirmed reduction, and is examined further through the flow field analyses presented in the following subsections.

a. Flow Velocity Contour Analysis

To further examine the hydrodynamic mechanisms underlying the observed resistance behavior, the flow field around the hull is analyzed using flow velocity contour distributions. This analysis provides insight into how the bilge keel's presence influences local flow acceleration, boundary layer development, and wake structure relative to the bare hull configuration.

The flow velocity contour in the bilge region was examined to assess the viscous flow behavior associated with bilge keel installation. For clarity, the comparison is presented at 9 knots, where local flow features are more pronounced and therefore suitable for qualitative assessment. The corresponding velocity contour distributions for the bare hull and bilge keel equipped configurations are shown in Figures 10–15.

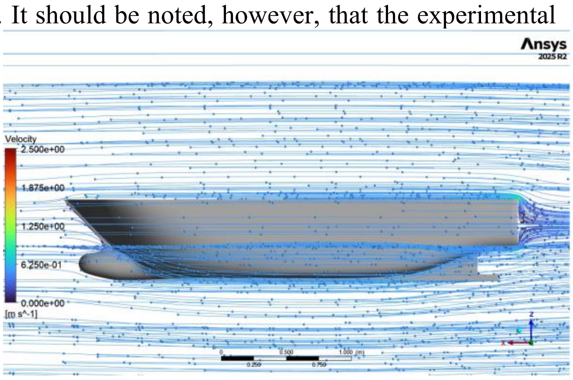

Figure 10. Flow Velocity Contour Bare Hull, 3 kn

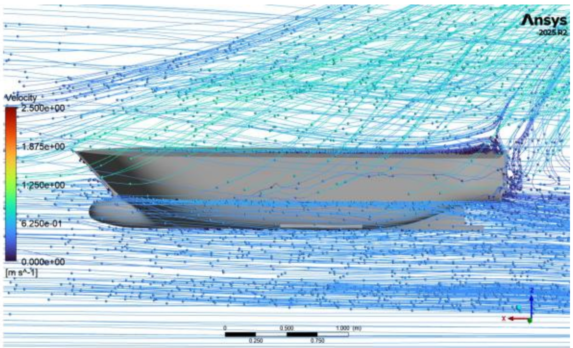

Figure 11. Flow Velocity Contour Bilge Keel, 3 kn

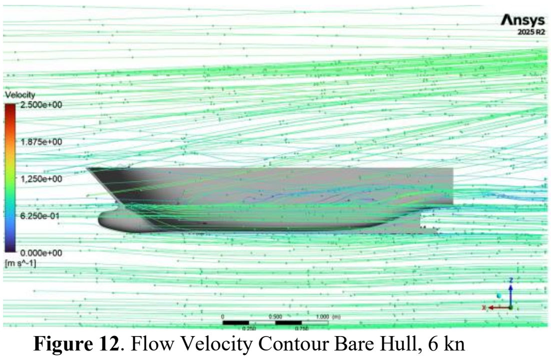

Figure 12. Flow Velocity Contour Bare Hull, 6 kn

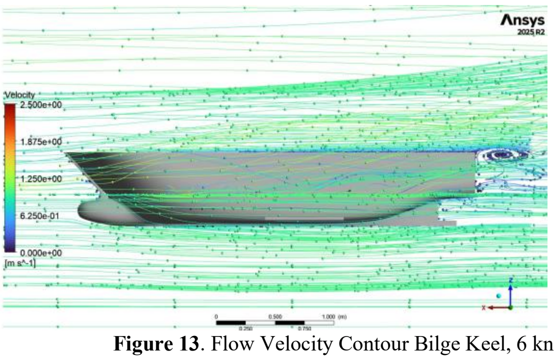

Figure 13. Flow Velocity Contour Bilge Keel, 6 kn

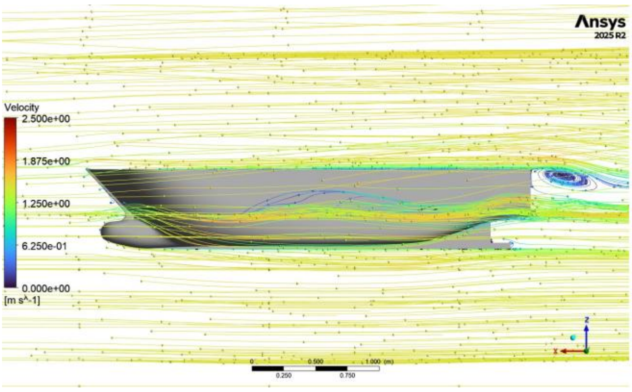

Figure 14. Flow Velocity Contour Bare Hull, 9 kn

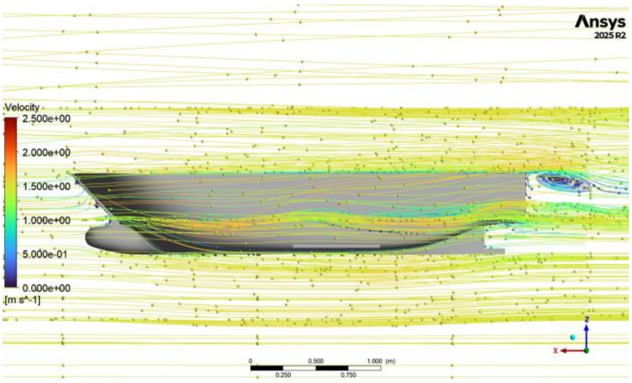

Figure 15. Flow Velocity Contour Bilge Keel, 9 kn

For the bare hull configuration, the velocity contours indicate the expected development of the boundary layer along the hull length, with a pronounced region of near wall flow acceleration occurring at the bilge turn as the flow follows the curved hull geometry. This localized acceleration is accompanied by closely packed streamlines adjacent to the hull surface, suggesting intensified velocity gradients that may contribute to increased viscous shear.

By contrast, the bilge keel configuration exhibits a clear redistribution of the local flow structure around the bilge region. The presence of the appendage modifies streamline trajectories, resulting in a more dispersed velocity field and a reduction in the localized acceleration observed for the bare hull case. Flow in this region appears less concentrated along the parent hull surface, indicating that momentum is distributed over a broader area rather than confined within a narrow near wall zone.

A further distinction is observed in the downstream region, where the wake behind the bilge keel configuration appears more structured compared to the bare hull case. This behavior suggests a smoother flow development toward the stern, which may improve flow recovery characteristics.

Despite the increase in wetted surface area and the Introduction of appendage related drag, the modified near wall flow behavior indicates that viscous effects cannot be evaluated solely on geometric grounds. Consideration must also be given to the interaction between the appendage and the surrounding boundary layer. This observation suggests a potential mechanism by which the bilge keel configuration may moderate friction related resistance under the present conditions.

This interpretation is based on a qualitative assessment of the velocity contour field rather than on direct wall shear stress evaluation. It therefore represents a flow based interpretation of the predicted results. The implications of these flow modifications are further examined through pressure contour analysis, with particular focus on the associated pressure distribution along the hull surface.

b. Pressure Contour Analysis

The pressure contours obtained for the bare hull configuration exhibit the characteristic pressure distribution expected for a conventional displacement vessel advancing in calm water. The corresponding pressure contour visualizations for both hull configurations at the investigated operating speeds are presented in Figures 16–21. High pressure regions are concentrated at the forward stagnation zone near the bow, where incoming flow decelerates upon encountering the hull surface, followed by a progressive pressure decrease along the midship region as the flow accelerates around the hull geometry. Moving toward the stern, the pressure field gradually recovers as the flow decelerates along the aft body.

Despite this general pattern, the aft bilge region exhibits a comparatively sharper pressure transition relative to the surrounding hull surface, particularly at higher operating speeds. This behavior is reflected in the closely spaced contour lines and the rapid variation between high and low pressure regions, indicating a stronger adverse pressure gradient as the flow negotiates the curvature from the bilge toward the stern. Such a localized pressure transition is commonly associated with less favorable stern flow development and may contribute to increased pressure related resistance.

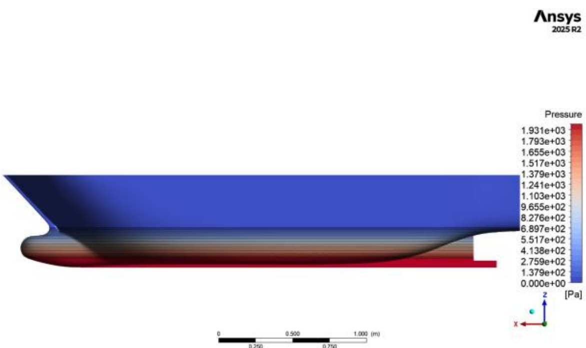

Figure 16. Pressure Contour Bare Hull, 3 kn

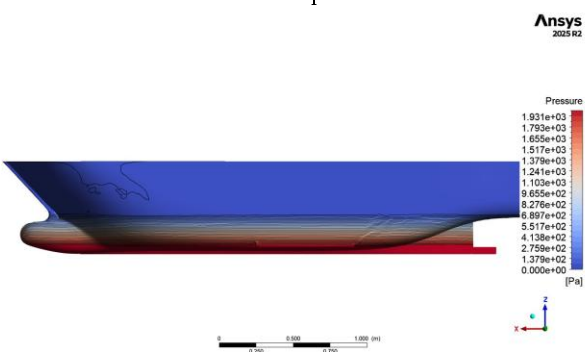

Figure 17. Pressure Contour Bilge Keel, 3 kn

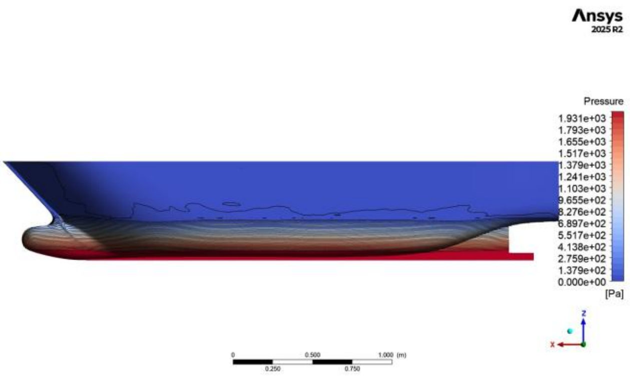

Figure 18. Pressure Contour Bare Hull, 6 kn

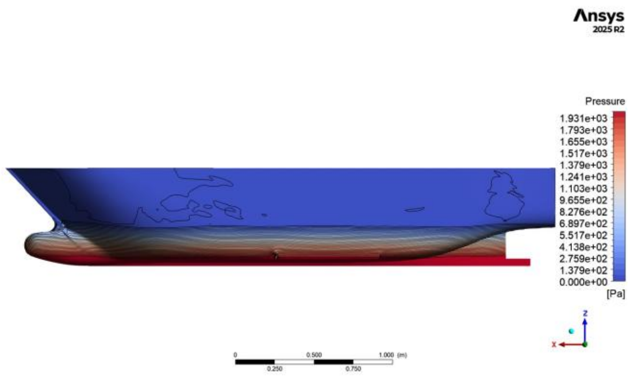

Figure 19. Pressure Contour Bilge Keel, 6 kn

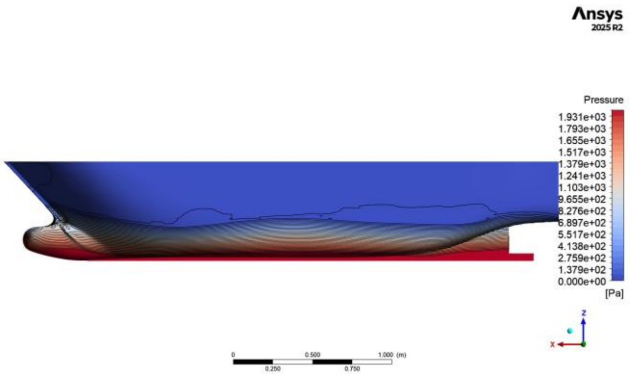

Figure 20. Pressure Contour Bare Hull, 9 kn

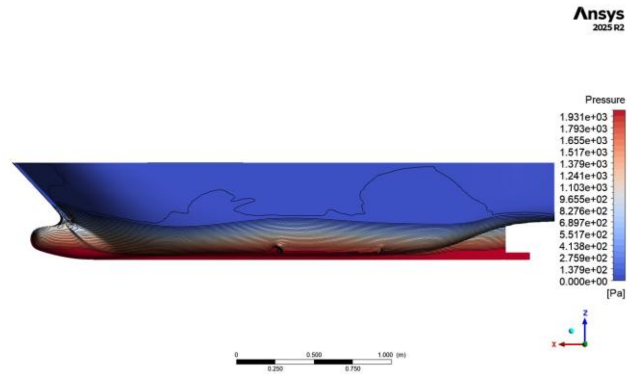

Figure 21. Pressure Contour Bilge Keel, 9 kn

For the bilge keel equipped configuration, the overall pressure field retains the same global distribution as the bare hull, indicating that the appendage's installation does not fundamentally alter the vessel's primary displacement flow characteristics. Nevertheless, localized modifications of the pressure contours are clearly observed in the vicinity of the bilge keel and the adjacent aft body region.

Compared with the bare hull case, the pressure transition around the aft bilge appears more gradually distributed, as indicated by smoother contour spacing and less abrupt variation between high and low pressure regions. That suggests that the bilge keel modifies the local flow development, redistributing pressure more progressively over the bilge turn and the lower stern region. The effect becomes more pronounced with increasing vessel speed, indicating stronger interaction between the appendage and the surrounding flow at higher momentum conditions.

From a hydrodynamic perspective, a more gradual pressure recovery is generally associated with reduced severity of adverse pressure gradients and may therefore contribute to a lower pressure related resistance component. The observed pressure redistribution thus provides a plausible explanation for the reduced total resistance predicted for the bilge keel configuration. However, because the present assessment relies on qualitative contour interpretation rather than direct integration of the pressure coefficient, this explanation should be regarded as an inferred hydrodynamic interpretation. Taken together with the validated resistance results and the observed modifications in the velocity field, these findings indicate that the bilge keel influences both viscous and pressure related flow characteristics under the investigated configuration.

Bringing these observations together, the validated RANS based CFD framework applied to a tuna longline fishing vessel reconstructed from field survey data in Benoa predicts a consistent reduction in total resistance for the bilge keel equipped configuration. This outcome departs from the conventional expectation of an additional drag penalty. It addresses the research gap identified in the Introduction regarding the absence of validated hydrodynamic evidence for this class of Indonesian working vessel. The magnitude of the reduction, however, cannot yet be attributed to a single physical mechanism based solely on qualitative flow field interpretation, and the bilge keel configuration has not been compared with a dedicated experimental counterpart. This discrepancy constitutes the principal open research question arising from the study and warrants further investigation through quantitative decomposition of the resistance component, integration of pressure coefficients, parametric variation of bilge keel geometry, and dedicated experimental validation.

IV. CONCLUSION

This study used a validated RANS based CFD approach to examine the effect of bilge keel installation on the resistance characteristics of a tuna longline fishing vessel. The reliability of the simulation framework for resistance analysis was confirmed by the numerical model's initial validation against towing tank data, which demonstrated good agreement at the representative operating speeds, with deviations of 3.3% at 6 knots and 5.6% at 9 knots.

The findings show that installing a bilge keel affects the vessel's resistance behavior. The total resistance increases non linearly with speed in both configurations, but the resistance produced by the bilge keel equipped hull is consistently lower than that of the bare hull. At a design speed of 6 knots, approximately 18% is reduced, which is relevant to the vessel's operational efficiency. This outcome contrasts with the conventional expectation that bilge keel installation introduces an additional drag penalty due to increased wetted surface area.

Qualitative flow field analysis associates this decrease with smoother pressure recovery in the aft bilge region and a redistribution of near wall velocity. These observations indicate that the bilge keel's influence on resistance is governed by its interaction with the surrounding flow in addition to the increase in wetted surface area, implying that a favorable balance between pressure and viscous effects can occur for specific hull appendage configurations.

Within the limits of the investigated configuration, the present findings indicate that installing bilge keels results in lower total resistance and may offer hydrodynamic benefits beyond their conventional role in vessel stability, particularly for fishing vessels with comparable hull characteristics. Further investigation is recommended to address the open question identified above, in particular through quantitative decomposition of the frictional and pressure resistance components, integration of the pressure coefficient over the aft body, and dedicated experimental validation of the bilge keel equipped configuration.

ACKNOWLEDGEMENT

The authors acknowledge the Hydrodynamics Technology Research Center, National Research and Innovation Agency (BRIN), Surabaya, Indonesia, for providing the vessel data, simulation facilities, and technical support that contributed to this research. The authors also acknowledge the Department of Marine Engineering, Universitas Pembangunan Nasional Veteran Jakarta, Indonesia, for the academic support provided during the completion of this study.

REFERENCES

[1] G. J. Grigoropoulos, "Hydrodynamic Design of Ships," *J. Mar. Sci. Eng.*, vol. 10, no. 4, pp. 8–11, 2022, doi: 10.3390/jmse10040512.

[2] International Maritime Organization (IMO), "2023 IMO Strategy on Reduction of GHG Emissions from Ships," *MEPC 80/WP.12, Annex.*, 2023.

[3] J. W. Yu, M. K. Lee, Y. I. Kim, S. B. Suh, and I. Lee, "An optimization study on the hull form and stern appendage for improving resistance performance of a coastal fishing vessel," *Appl. Sci.*, vol. 11, no. 13, 2021, doi: 10.3390/app11136124.

[4] S. H. Lee, H. Kim, and S. Kwon, "Fishing Vessel Risk and Safety Analysis: A Bibliometric Analysis, Clusters Review and Future Research Directions," *Appl. Sci.*, vol. 14, no. 22, pp. 1–34, 2024, doi: 10.3390/app142210439.

[5] E. S. Putra, E. C. Ilman, and A. Fitriadhy, "Computational Investigation into Bilge Keel Effect on a Traditional Phinisi Boat's Resistance," *J. Sh. Mar. ...*, vol. 1, no. 1, pp. 23–32, 2023, [Online]. Available: https://semarakilmu.com.my/journals/index.php/jsms/article/view/4904%0Ahttps://semarakilmu.com.my/journals/index.php/jsms/article/download/4904/2699

[6] M. M. Sarker and M. Tarafder, "CFD based investigation of appendage effects on ship resistance and flow characteristics," *Ocean Eng.*, vol. 285, 2024.

[7] S. Oyuela, H. R. D. Ojeda, F. P. Arribas, A. D. Otero, and R. Sosa, "Investigating Fishing Vessel Hydrodynamics by Using EFD and CFD Tools, with Focus on Total Ship Resistance and Its Components," *J. Mar. Sci. Eng.*, vol. 12, no. 4, pp. 1–18, 2024, doi: 10.3390/jmse12040622.

[8] M. S. R. Hamka, Y. Novita, and V. R. Kurniawati, "The Impact of B/D Ratio on the Technical Performance of Outrigger Fishing Vessels at PPN Palabuhanratu," *Int. J. Mar. Eng. Innov. Res.*, vol. 9, no. 1, pp. 200–207, 2024, doi: 10.12962/j25481479.v9i1.20214.

[9] H. Harifuddin, I. M. Ariana, and B. Cahyono, "Effect of Rudder Bulb Installation on Ship Propulsion Performance of Anchor Handling Design VS 491 CD during Towing Barge Operation," *Int. J. Mar. Eng. Innov. Res.*, vol. 8, no. 3, pp. 422–429, 2023, doi: 10.12962/j25481479.v8i3.17703.

[10] I. Sulovsky, G. de Hauteclocque, M. Greco, and J. Prpić-Oršić, "Comparative Study of Potential Flow and CFD in the Assessment of Seakeeping and Added Resistance of Ships," *J. Mar. Sci. Eng.*, vol. 11, no. 3, 2023, doi: 10.3390/jmse11030641.

[11] E. Begovic, C. Bertorello, R. Ponzini, and F. Salvadore, "Planing Hull Hydrodynamic Performance Prediction Using LincoSim Virtual Towing Tank," *J. Mar. Sci. Eng.*, vol. 12, no. 5, 2024, doi: 10.3390/jmse12050794.

[12] N. J. van der Kolk, I. Akkerman, J. A. Keuning, and R. H. M. Huijsmans, "Low-aspect ratio appendages for wind-assisted ships," *J. Mar. Sci. Technol.*, vol. 26, no. 4, pp. 1126–1143, 2021, doi: 10.1007/s00773-020-00777-8.

[13] Y. Wang, H. Rao, Z. Liu, K. Liu, B. Zhou, and G. Zhang, "Numerical Prediction of Ship Resistance Based on Volume of Fluid Implicit Multi-Step Method," *J. Mar. Sci. Eng.*, vol. 11, no. 11, 2023, doi: 10.3390/jmse11112181.

[14] P. C. Wu, "A CFD-Based Correction for Ship Mass and Longitudinal Center of Gravity to Improve Resistance Simulation," *Mathematics*, vol. 13, no. 11, 2025, doi: 10.3390/math13111788.

[15] J. Zhou, J. Ren, C. Tu, and S. Yang, "Numerical Investigation of Flow Field Characteristics around Two Ship Hull Sections with Different Reynolds Numbers," *J. Mar. Sci. Eng.*, vol. 12, no. 9, 2024, doi: 10.3390/jmse12091547.

[16] A. Trimulyono, M. F. Nuralam, D. Chrismianto, S. Samuel, I. P. Mulyatno, and M. Iqbal, "Investigation of Planing Hull Resistance Calculation Using Smoothed Particle Hydrodynamics," *Int. J. Mar. Eng. Innov. Res.*, vol. 10, no. 2, pp. 329–333, 2025, doi: 10.12962/j25481479.v10i2.6373.

[17] M. Mousaviraad, A. M. Ghassemi, and H. Nowruzi, "Adaptive Grid Refinement for Ship Resistance Computations," *Ocean Eng.*, vol. 250, 2022.

[18] Y. Tian *et al.*, "A Comparative CFD Study on the Wave-Making Characteristics and Resistance Performance of Two Representative Naval Vessel Designs," *J. Mar. Sci. Eng.*, vol. 14, no. 2, p. 212, 2026, doi: 10.3390/jmse14020212.

[19] Y. Wan, Y. Hou, C. Gong, Y. Zhang, Y. Zhang, and Y. Xiong, "Hydrodynamic Performance Analysis of a Submersible Surface Ship and Resistance Forecasting Based on BP Neural Networks," *J. Mar. Sci. Appl.*, vol. 21, no. 2, pp. 34–46, 2022, doi: 10.1007/s11804-022-00278-7.

[20] Y. Feng, O. el Moctar, and T. E. Schellin, "Parametric Hull Form Optimization of Containerships for Minimum Resistance in Calm Water and in Waves," *J. Mar. Sci. Appl.*, vol. 20, no. 4, pp. 670–693, 2021, doi: 10.1007/s11804-021-00243-w.

[21] A. Mandru and F. Pacuraru, "The effect of appendages on ship resistance," *IOP Conf. Ser. Mater. Sci. Eng.*, vol. 1182, no. 1, p. 012041, 2021, doi: 10.1088/1757-899x/1182/1/012041.

[22] D. Purnamasari, M. R. Utina, Rina, E. Suwarni, "Model experiment on fishing vessel operation in Benoa, Bali, using wind-assisted propulsion system," *Res. Rep., BRIN, Surabaya, Indones.*, 2025.

[23] A. M. Elhadad, A. M. A. El-Ela, and M. M. Hussien, "Investigation of the Influence of Bulbous Bow on the Wake Field and Power Demand," *J. Adv. Res. Fluid Mech. Therm. Sci.*, vol. 123, no. 2, pp. 140–152, 2024, doi: 10.37934/arfmts.123.2.140152.